Journal of Biomolecular Structure and Dynamics

ISSN: (Print) (Online) Journal homepage: https://www.tandfonline.com/loi/tbsd20

Synthesis, antimicrobial properties and *in silico* studies of aryloxyacetic acid derivatives with hydrazone or thiazolidine-4-one scaffold

Sevil Şenkardeş, Didem Kart, Bilge Bebek, Miyase Gözde Gündüz & Ş Güniz Küçükgüzel

To cite this article: Sevil Şenkardeş, Didem Kart, Bilge Bebek, Miyase Gözde Gündüz & Ş Güniz Küçükgüzel (2022): Synthesis, antimicrobial properties and *in silico* studies of aryloxyacetic acid derivatives with hydrazone or thiazolidine-4-one scaffold, Journal of Biomolecular Structure and Dynamics, DOI: 10.1080/07391102.2022.2121761

To link to this article: https://doi.org/10.1080/07391102.2022.2121761

JOURNAL OF BIOMOLECULAR STRUCTURE AND DYNAMICS
https://doi.org/10.1080/07391102.2022.2121761

Synthesis, antimicrobial properties and *in silico* studies of aryloxyacetic acid derivatives with hydrazone or thiazolidine-4-one scaffold

Sevil Şenkardeş[a], Didem Kart[b], Bilge Bebek[a,c], Miyase Gözde Gündüz[d] and Ş Güniz Küçükgüzel[e]

[a]Department of Pharmaceutical Chemistry, Faculty of Pharmacy, Maltepe, Marmara University, Başıbüyük, İstanbul, Turkey; [b]Department of Pharmaceutical Microbiology, Faculty of Pharmacy, Hacettepe University, Sıhhiye, Ankara, Turkey; [c]Deva Holding A.S., R & D Center, Cerkezkoy, Tekirdag, Turkey; [d]Department of Pharmaceutical Chemistry, Faculty of Pharmacy, Hacettepe University, Sıhhiye, Ankara, Turkey; [e]Department of Pharmaceutical Chemistry, Faculty of Pharmacy, Fenerbahçe University, Ataşehir, İstanbul, Turkey

Communicated by Ramaswamy H. Sarma

ABSTRACT

In this work, twenty hydrazide-hydrazone and 4-thiazolidinone derivatives were synthesized starting from m-cresol. Antimicrobial evaluation was carried out by microdilution method against *Enterococcus faecalis* and *Staphylococcus aureus* as Gram-positive bacteria and *Escherichia coli* and *Pseudomonas aeruginosa* as Gram-negative bacteria, and three pathogenic fungi *Candida albicans*, *Candida parapsilosis* and *Candida krusei*. Some compounds possessed considerable antimicrobial properties against the tested microorganisms, particularly against *E. coli*. 4-Thiazolidinones containing 3-methoxyphenyl and 3,5-dichlorophenyl moieties (**4h** and **4i**) were found to be the most active derivatives with MICs of 2 μg/mL against *E. coli*. *N*′-[(3,5-dichlorophenyl)methylidene]-2-(3-methylphenoxy)acetohydrazide (**3i**) also displayed antifungal activity against *Candida krusei* that was comparable to fluconazole. Calculated drug-likeness and ADMET parameters of the most active compounds confirmed their potential as antimicrobial drug candidates. Molecular docking investigations were carried out in the thiamine diphosphate-binding site of pyruvate dehydrogenase multienzyme complex E1 component (PDHc-E1) to clarify the potential antibacterial mechanism against *E. coli*. The results showed the potential and importance of developing new hydrazones and 4-thiazolidinones that would be effective against microbial strains.

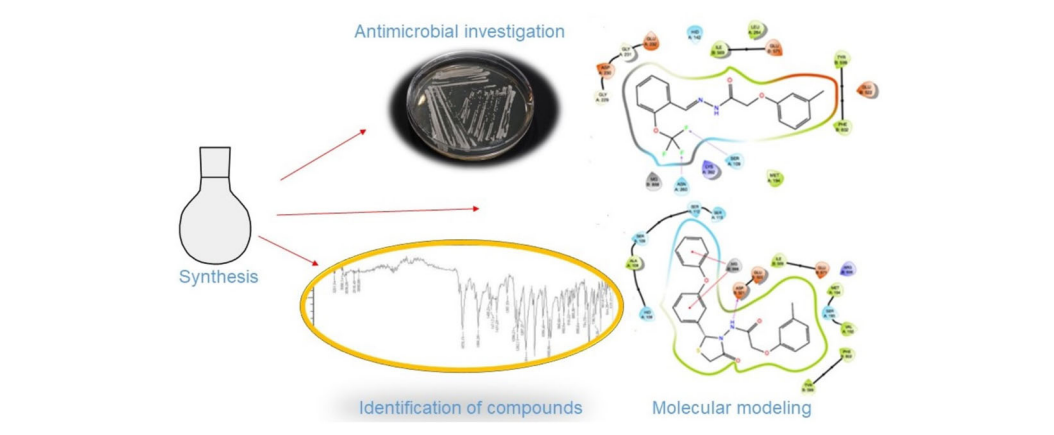

ARTICLE HISTORY
Received 27 May 2022
Accepted 31 August 2022

KEYWORDS
Cresol; hydrazone; 4-thiazolidinone; molecular docking; antimicrobial activity

1. Introduction

Antimicrobial resistance (AMR)—that occurs when microorganisms become resistant to the effects of antimicrobials—is recognized as one of the prominent global public health threats in the 21st century. According to The Lancet's most comprehensive analysis on bacterial AMR to date, while 4.95 million people died in 2019 because of antibiotic-resistant bacterial infections, 1.27 million people died directly as a result of AMR (Murray et al., 2022). Antimicrobials, notably antibiotics, have been the keystone in modern medicine. The discovery of antibiotics and their usage in the treatment of infectious diseases worldwide eventually have been regarded as a revolution (Gajdács & Albericio, 2019). Although all beneficial outcomes of

CONTACT Sevil Şenkardeş sevil.aydin@marmara.edu.tr Department of Pharmaceutical Chemistry, Faculty of Pharmacy, Marmara University, Başıbüyük, İstanbul 34854, Turkey.

Supplemental data for this article can be accessed online at https://doi.org/10.1080/07391102.2022.2121761

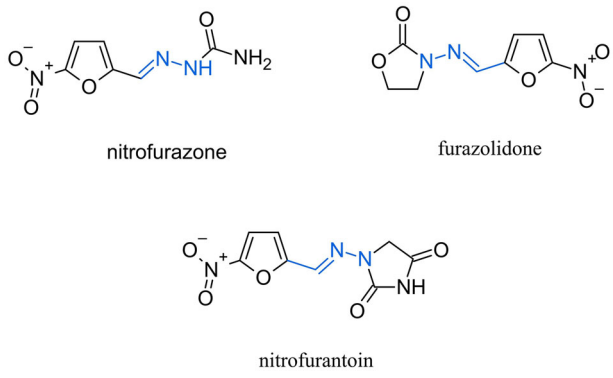

Figure 1. Hydrazone based antimicrobial drugs.

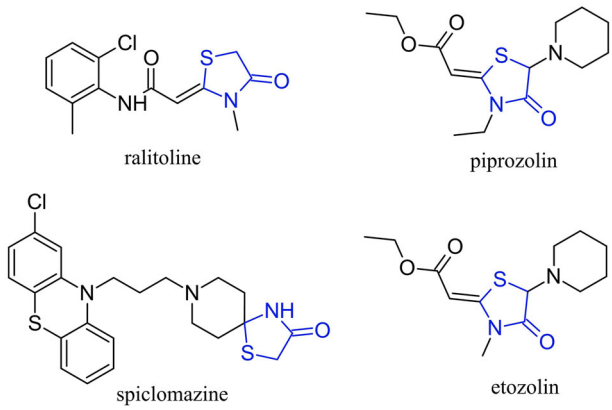

Figure 2. Some commercially available drugs bearing 4-thiazolidinone ring.

antimicrobials in the process of dealing with bacterial infections, over the years their effectiveness has started to decrease due to the evolution of bacterial resistance in these pathogens, making the need for the new generation of antimicrobials more urgent to reduce the spread of antibiotic resistance (de la Fuente-Nunez et al., 2017; Laxminarayan et al., 2016). For instance, *Escherichia coli* is a typical commensal of the vaginal and skin microbiota, as well as the stomach (Sharma et al., 2022). Due to the development of resistance to the majority of mostly used antimicrobial drugs (e.g., amoxicillin, cefixime, and ciprofloxacin), the management of *E. coli* infections has grown more challenging (Laxminarayan et al., 2013). It is therefore also necessary to develop new agents with excellent antibacterial effects against drug-resistant clinical pathogens such as *E. coli*, *S. aureus* and *K. pneumonia* (Mccarthy et al., 2020).

Hydrazones are a significant class of organic compounds because of not only their biological activities but also azomethine group (–NH–N = CH–) attached to the carbonyl functionality, which allows applying various synthetic routes to reach various heterocyclic scaffolds, such as 4-thiazolidinones (Rollas & Küçükgüzel, 2007). Hydrazone moiety is also present in the chemical structure of medicines with antimicrobial activity (Küçükgüzel et al., 2002, 2003), such as nitrofurazone, furazolidone, or nitrofurantoin (Figure 1).

In medicinal chemistry, heterocyclic scaffolds are known for their great importance. It has been proved that more than 85% of all chemical entities which have biological activity include at least one heterocycle (Jampilek, 2019). 4-Thiazolidinones are one of the most important five-membered heterocyclic rings, which attracted special interest over the years with their chemical structure containing one nitrogen and one sulfur atom, as well as a C = O group at the 4-position. It has been reported that while substituents in the other positions may be varied, the difference in the properties is mainly provided by the group attached to the carbon in the 2-position (Verma & Saraf, 2008). They are associated with their broad biological activities, such as antitumoral (Cikla et al., 2013; Han et al., 2021; Koç et al., 2022; Şenkardeş & Kucukguzel, 2016), antidiabetic (Datar & Aher, 2016), antiinflammatory (Shawky et al., 2020), antiviral (Kaushik-Basu et al., 2008), and antitubercular (Küçükgüzel et al., 2006). The following thiazolidinone-based compounds are used as registered drugs: ralitoline (anticonvulsant), piprozolin (choleretic), etozolin (antihypertensive, diuretic), spiclomazine (psychotropic) (Figure 2). In addition, the researchers have determined by molecular modeling that some structures containing hydrazone and thiazolidone inhibit potential target enzymes of SARS-CoV-2 (Şahin et al., 2021).

The valuable biological activities of hydrazone and 4-thiazolidinone based compounds prompted us to synthesize new derivatives. In continuation of our work on these moieties, we have evaluated the antimicrobial activities of a series of hydrazones and 4-thiazolidinones derived from m-cresol and supported the obtained biological results by computational techniques.

2. Materials and methods

2.1. Chemistry

All melting points are recorded on digital Electrothermal Thermo Scientific IA9300 instrument and are uncorrected. The IR spectra (cm^{-1}) was characterized on a Fourier transform infrared spectrometer (FTIR, 8400S, Shimadzu, Japan). ^{1}H and ^{13}C-NMR spectra were recorded in $CDCl_3$ and/or DMSO-d_6 on BRUKER NMR spectrometer and are reported relative to deuterated solvent signals. Elemental microanalysis was carried out on a CHNS-932 (LECO) analyzer.

2.1.1. Preparation of ethyl (3-methylphenoxy)acetate (1)

m-Cresol, also 3-methylphenol, (0.06 mol) and K_2CO_3 (0.09 mol) were dissolved in anhydrous acetone and the mixture was refluxed for 4 h. Then ethyl bromoacetate (0.063 mol) was added dropwise and refluxed with stirring for 5–8 h. Evaporation of the acetone gave oily compound **1** (Del Carmen Cruz et al., 2003).

2.1.2. Preparation of 2-(3-methylphenoxy)acetohydrazide (2)

Heating compound **1** (0.01 mol) with hydrazine hydrate (5 mL, 80%) under the reflux in 20 ml ethanol for 2–5 h led to the formation of compound **2**. The obtained solid was recrystallized from ethanol (Sathisha et al., 2011).

2.1.3. Synthesis of N′-[(substituted aromatic)methylidene]-2-(3-methylphenoxy)acetohydrazide (3a-j)

Equimolar quantity of 2-(3-methylphenoxy)acetohydrazide **(2)** (0.003 mol) and various aldehydes (0.003 mol) were dissolved in ethanol then refluxed for 3–5 h using glacial acetic acid as a catalyst. The mixture was cooled and solid obtained was filtered, recrystallized from ethanol.

N′-[(2-chloro-3-methoxyphenyl)methylidene]-2-(3-methylphenoxy)acetohydrazide (3a). White solid; yield: 73%; mp 163 °C; FTIR (v, cm^{-1}): 3201 (N-H), 1678 (C = O), 1596 (C = N); ^{1}H-NMR (300 MHz), (DMSO-d_6/TMS) δ ppm: 2.27 & 2.29 (ss, 3H, Ar-C**H**$_3$), 4.65 & 5.13 (ss, 2H, O-C**H**$_2$), 6.84-7.61 (m, 7H, Ar-**H**), 8.43 & 8.77 (ss, 1H, C**H**=N), 11.79 (s, 1H, CO-N**H**); ^{13}C-NMR ($CDCl_3$, 100 MHz) δ ppm: 20.5 (Ar-**C**H$_3$), 55.3 (-O**C**H$_3$), 64.4 & 66.1 (-O**C**H$_2$), 144.8 & 140.7 (-**C = N**), 154.1 (=**C**H-OCH$_2$), 155.9 (=**C**H-OCH$_3$), 163.6 (-**C = O**); Anal. Calcd. for $C_{17}H_{17}ClN_2O_3$.1/4 H_2O: C, 60.54; H, 5.23; N, 8.31; found: C, 60.90; H, 4.93; N, 8.41%.

N′-{2-chloro-3-(trifluoromethyl)phenyl]methylidene}-2-(3-methylphenoxy)acetohydrazide (3b). Off-white solid; yield: 81%; mp 150–151 °C; FTIR (v, cm^{-1}): 3196 (N-H), 1678 (C = O), 1587 (C = N); ^{1}H-NMR (300 MHz), (DMSO-d_6/TMS) δ ppm: 2.27 & 2.29 (ss, 3H, Ar-C**H**$_3$), 4.68 & 5.16 (ss, 2H, O-C**H**$_2$), 6.79-8.33 (m, 7H, Ar-**H**), 8.49 & 8.87 (ss, 1H, C**H**=N), 11.92 (s, 1H, CO-N**H**); ^{13}C-NMR ($CDCl_3$, 100 MHz) δ ppm: 21.6 (Ar-**C**H$_3$), 65.5 & 67.2 (-O**C**H$_2$), 144.6 & 140.3 (-**C = N**), 157.0 (=**C**H-OCH$_2$), 165.0 (-**C = O**); Anal. Calcd. for $C_{17}H_{14}ClF_3N_2O_2$: C, 55.07; H, 3.81; N, 7.56; found: C, 55.08; H, 3.53; N, 7.49%.

N′-[(4-fluoro-3-phenoxyphenyl)methylidene]-2-(3-methylphenoxy)acetohydrazide (3c). White solid; yield: 84%; mp 148–149 °C; FTIR (v, cm^{-1}): 3192 (N-H), 1674 (C = O), 1581 (C = N); ^{1}H-NMR (300 MHz), (DMSO-d_6/TMS) δ ppm: 2.26 & 2.28 (ss, 3H, Ar-C**H**$_3$), 4.62 & 5.04 (ss, 2H, O-C**H**$_2$), 6.66–7.58 (m, 12H, Ar-**H**), 7.97 & 8.29 (ss, 1H, C**H**=N), 11.61 (s, 1H, CO-N**H**); ^{13}C-NMR ($CDCl_3$, 100 MHz) δ ppm: 21.6 (Ar-**C**H$_3$), 65.3 & 67.2 (-O**C**H$_2$), 144.2 & 148.0 (-**C = N**), 156.8 (=**C**H-O-phenyl), 157.0 (=**C**H-OCH$_2$), 164.7 & 171.1 (-**C = O**); Anal. Calcd. for $C_{22}H_{19}FN_2O_3$: C, 69.83; H, 5.06; N, 7.40; found: C, 69.72; H, 5.02; N, 7.40%.

N′-[(3-phenoxyphenyl)methylidene]-2-(3-methylphenoxy)-acetohydrazide (3d). Off-white solid; yield: 85%; mp 110–111 °C; FTIR (v, cm^{-1}): 3194 (N-H), 1678 (C = O), 1573 (C = N); ^{1}H-NMR (300 MHz), (DMSO-d_6/TMS) δ ppm: 2.26 & 2.28 (ss, 3H, Ar-C**H**$_3$), 4.63 & 5.06 (ss, 2H, O-C**H**$_2$), 6.69–8.32 (m, 13H, Ar-**H**), 7.99 & 8.32 (ss, 1H, C**H**=N), 11.58 & 11.63 (ss, 1H, CO-N**H**); ^{13}C-NMR ($CDCl_3$, 100 MHz) δ ppm: 21.6 (Ar-**C**H$_3$), 65.3 & 67.3 (-O**C**H$_2$), 145.3 & 149.1 (-**C = N**), 156.7 & 156.9 (=**C**H-O-phenyl), 157.1 & 157.8 (=**C**H-O-phenyl), 157.9 & 158.2 (=**C**H-OCH$_2$), 164.8 & 171.2 (-**C = O**); Anal. Calcd. for $C_{22}H_{20}N_2O_3$: C, 73.32; H, 5.59; N, 7.77; found: C, 73.51; H, 5.57; N, 7.79%.

2-(3-Methylphenoxy)-N′-[(4-phenylthiophen-2-yl)methylidene]acetohydrazide (3e). Off-white solid; yield: 69%; mp 204–205 °C; FTIR (v, cm^{-1}): 3196 (N-H), 1678 (C = O), 1587 (C = N); ^{1}H-NMR (300 MHz), (DMSO-d_6/TMS) δ ppm: 2.27 & 2.29 (ss, 3H, Ar-C**H**$_3$), 4.64 & 5.04 (ss, 2H, O-C**H**$_2$), 6.83–7.99 (m, 11H, Ar-**H**), 8.24 & 8.59 (ss, 1H, C**H**=N), 11.62 (s, 1H, CO-N**H**); ^{13}C-NMR ($CDCl_3$, 100 MHz) δ ppm: 21.7 (Ar-**C**H$_3$), 64.8 & 66.9 (-O**C**H$_2$), 140.2 & 143.3 (-**C = N**), 158.3 & 158.7 (=**C**H-OCH$_2$), 164.8 & 169.3 (-**C = O**); Anal. Calcd. for $C_{20}H_{18}N_2O_2S$: C, 68.55; H, 5.18; N, 7.99; S, 9.15; found: C, 68.12; H, 5.65; N, 8.11; S, 9.51%.

2-(3-Methylphenoxy)-N′-{[4-(trifluoromethoxy)phenyl]methylidene}acetohydrazide (3f). White solid; yield: 92%; mp 141 °C; FTIR (v, cm^{-1}): 3192 (N-H), 1680 (C = O), 1610 (C = N); ^{1}H-NMR (300 MHz), (DMSO-d_6/TMS) δ ppm: 2.27 & 2.29 (ss, 3H, Ar-C**H**$_3$), 4.65 & 5.12 (ss, 2H, O-C**H**$_2$), 6.82–7.87 (m, 8H, Ar-**H**), 8.04 & 8.38 (ss, 1H, C**H**=N), 11.67 (s, 1H, CO-N**H**); ^{13}C-NMR ($CDCl_3$, 100 MHz) δ ppm: 21.6 (Ar-**C**H$_3$), 65.4 & 67.3 (-O**C**H$_2$), 144.4 & 147.3 (-**C = N**), 150.6 & 150.9 (=**C**H-OCF$_3$), 157.1 & 158.2 (=**C**H-OCH$_2$), 164.9 & 171.2 (-**C = O**); Anal. Calcd. for $C_{17}H_{15}F_3N_2O_3$: C, 57.96; H, 4.29; N, 7.95; found: C, 57.83; H, 4.02; N, 7.96%.

N′-[(4-fluoro-3-methoxyphenyl)methylidene]-2-(3-methylphenoxy)acetohydrazide (3g). White solid; yield: 87%; mp 146 °C; FTIR (v, cm^{-1}): 3180 (N-H), 1678 (C = O), 1612 (C = N); ^{1}H-NMR (300 MHz), (DMSO-d_6/TMS) δ ppm: 2.27 & 2.29 (ss, 3H, Ar-C**H**$_3$), 3.88 (s, 3H, -OCH$_3$), 4.64 & 5.13 (ss, 2H, O-C**H**$_2$), 6.82–7.51 (m, 7H, Ar-**H**), 7.98 & 8.31 (ss, 1H, C**H**=N), 11.53 & 11.58 (ss, 1H, CO-N**H**); Anal. Calcd. for $C_{17}H_{17}FN_2O_3$. 1/4H_2O: C, 63.64; H, 5.50; N, 8.73; found: C, 63.96; H, 5.14; N, 8.88%.

2-(3-Methylphenoxy)-N′-{[2-(trifluoromethoxy)phenyl]methylidene}acetohydrazide (3h). Off-white solid; yield: 84%; mp 118–120 °C; FTIR (v, cm^{-1}): 3228 (N-H), 1674 (C = O), 1606 (C = N); ^{1}H-NMR (300 MHz), (DMSO-d_6/TMS) δ ppm: 2.27 & 2.29 (ss, 3H, Ar-C**H**$_3$), 4.66 & 5.14 (ss, 2H, O-C**H**$_2$), 6.71-8.09 (m, 8H, Ar-**H**), 8.28 & 8.64 (ss, 1H, C**H**=N), 11.74 & 11.83 (ss, 1H, CO-N**H**); ^{13}C-NMR ($CDCl_3$, 100 MHz) δ ppm: 21.6 (Ar-**C**H$_3$), 65.5 & 67.3 (-O**C**H$_2$), 142.8 & 147.9 (-**C = N**), 157.1 (=**C**H-OCF$_3$), 158.2 (=**C**H-OCH$_2$), 164.8 & 170.2 (-**C = O**); Anal. Calcd. for $C_{17}H_{15}F_3N_2O_3$: C, 57.96; H, 4.29; N, 7.95; found: C, 58.06; H, 3.99; N, 8.01%.

N′-[(3,5-dichlorophenyl)methylidene]-2-(3-methylphenoxy)acetohydrazide (3i). White solid; yield: 93%; mp 168–169 °C; FTIR (v, cm^{-1}): 3178 (N-H), 1680 (C = O), 1614 (C = N); ^{1}H-NMR (300 MHz), (DMSO-d_6/TMS) δ ppm: 2.27 & 2.29 (ss, 3H, Ar-C**H**$_3$), 4.66 & 5.16 (ss, 2H, O-C**H**$_2$), 6.71–7.79 (m, 7H, Ar-**H**), 7.97 & 8.29 (ss, 1H, C**H**=N), 11.79 & 11.84 (ss, 1H, CO-N**H**); ^{13}C-NMR ($CDCl_3$, 100 MHz) δ ppm: 21.7 (Ar-**C**H$_3$), 65.1 & 66.8 (-O**C**H$_2$), 141.3 & 145.2 (-**C = N**), 158.2 & 158.7 (=**C**H-OCH$_2$), 165.3 & 170.1 (-**C = O**); Anal. Calcd. for $C_{16}H_{14}Cl_2N_2O_2$: C, 56.99; H, 4.18; N, 8.31; found: C, 56.96; H, 3.88; N, 8.43%.

N′-[(3,4-dimethylphenyl)methylidene]-2-(3-methylphenoxy)acetohydrazide (3j). Off-white solid; yield: 90%; mp 155–156 °C; FTIR (v, cm^{-1}): 3188 (N-H), 1681 (C = O), 1606 (C = N); ^{1}H-NMR (300 MHz), (DMSO-d_6/TMS) δ ppm: 2.25–2.29

(m, 9H, Ar-C**H**$_3$), 4.62 & 5.10 (ss, 2H, O-C**H**$_2$), 6.77–7.48 (m, 7H, Ar-**H**), 7.95 & 8.26 (ss, 1H, C**H**=N), 11.48 & 11.50 (ss, 1H, CO-N**H**); ^{13}C-NMR ($CDCl_3$, 100 MHz) δ ppm: 19.7 (Ar-**C**H$_3$), 20.0 (Ar-**C**H$_3$), 21.6 (Ar-**C**H$_3$), 65.5 & 67.3 (-O**C**H$_2$), 146.2 & 149.9 (**C = N**), 157.2 & 158.4 (=**C**H-OCH$_2$), 164.5 & 170.9 (-**C = O**); Anal. Calcd. for $C_{18}H_{20}N_2O_2$: C, 72.95; H, 6.80; N, 9.45; found: C, 72.72; H, 6.39; N, 9.38%.

2.1.4. Synthesis of N-[2-(substituted aryl)-4-oxo-1,3-thiazolidin-3-yl]-2-(3-methylphenoxy)acetamide (4a-j)

A mixture of hydrazone derivatives **(3a-j)** (0.001 mol) and thioglicolic acid (0.0012 mol) in toluene (80-100 ml) was refluxed using *Dean-Stark* apparatus for 10–12 h. After distillation of toluene, the separated product was crystallized from ethanol-water to give compounds **4a-j**.

N-[2-(2-chloro-3-methoxyphenyl)-4-oxo-1,3-thiazolidin-3-yl]-2-(3-methylphenoxy)acetamide (4a). Off-white solid; yield: 61%; mp 137–139 °C; FTIR (v, cm^{-1}) = 3200 (N-H), 1714 & 1681 (C = O); ^{1}H-NMR (300 MHz), (DMSO-d_6/TMS) δ ppm: 2.26 (s, 3H, Ar-C**H**$_3$), 3.73-3.92 (m, 5H, thiazolidinone C**H**$_2$ heterocycle & Ar-OC**H**$_3$), 4.55 (s, 2H, O-C**H**$_2$), 6.13 (s, 1H, S-C**H**-N), 6.63-7.41 (m, 7H, Ar-**H**), 10.65 (s, 1H, CO-N**H**); ^{13}C-NMR ($CDCl_3$, 100 MHz) δ ppm: 21.5 (Ar-**C**H$_3$), 29.7 (thia. **C**$_5$), 56.4 (Ar-O**C**H$_3$), 59.5 (thia. **C**$_2$), 67.1 (O**C**H$_2$), 155.6 (=**C**H-OCH$_2$), 156.8 (=**C**H-OCH$_3$), 167.1 (amide **C = O**), 169.9 (thia. C = O); Anal. Calcd. for $C_{19}H_{19}ClN_2O_4S$: C, 56.09; H, 4.71; N, 6.88; S, 7.88; found: C, 56.65; H, 4.49; N, 6.90; S, 7.92%.

N-[2-[2-chloro-3-(trifluoromethyl)phenyl]-4-oxo-1,3-thiazolidin-3-yl]-2-(3-methylphenoxy)acetamide (4b). White solid; yield: 58%; mp 191–192 °C; FTIR (v, cm^{-1}) = 3211 (N-H), 1714 & 1681 (C = O); ^{1}H-NMR (300 MHz), (DMSO-d_6/TMS) δ ppm: 2.20 (s, 3H, Ar-C**H**$_3$), 3.76-3.98 (m, 2H, thiazolidinone C**H**$_2$ heterocycle), 4.58 (s, 2H, O-C**H**$_2$), 6.19 (s, 1H, S-C**H**-N), 6.62-8.31 (m, 7H, Ar-**H**), 10.68 (s, 1H, CO-N**H**); ^{13}C-NMR ($CDCl_3$, 100 MHz) δ ppm: 21.5 (Ar-**C**H$_3$), 29.6 (thia. **C**$_5$), 59.1 (thia. **C**$_2$), 67.2 (O**C**H$_2$), 156.7 (=**C**H-OCH$_2$), 167.4 (amide **C = O**), 169.9 (thia. C = O); Anal. Calcd. for $C_{19}H_{16}ClF_3N_2O_3S$: C, 51.30; H, 3.63; N, 6.30; S, 7.21; found: C, 51.73; H, 3.86; N, 5.76; S, 6.82%.

N-[2-(4-fluoro-3-phenoxyphenyl)-4-oxo-1,3-thiazolidin-3-yl]-2-(3-methylphenoxy)acetamide (4c). White solid; yield: 50%; mp 178–179 °C; FTIR (v, cm^{-1}) = 3185 (N-H), 1714 & 1681 (C = O); ^{1}H-NMR (300 MHz), (DMSO-d_6/TMS) δ ppm: 2.24 (s, 3H, Ar-C**H**$_3$), 3.52–3.94 (dd, 2H, J = 15.6 Hz, thiazolidinone C**H**$_2$ heterocycle), 4.52 (s, 2H, O-C**H**$_2$), 5.81 (s, 1H, S-C**H**-N), 6.62-7.42 (m, 12H, Ar-**H**), 10.51 (s, 1H, CO-N**H**); ^{13}C-NMR ($CDCl_3$ & DMSO-d_6, 100 MHz) δ ppm: 21.6 (Ar-**C**H$_3$), 29.7 (thia. **C**$_5$), 61.4 (thia. **C**$_2$), 66.3 (O**C**H$_2$), 157.4 (=**C**H-F), 158.1 (=**C**H-OCH$_2$), 167.4 (amide **C = O**), 169.1 (thia. C = O); Anal. Calcd. for $C_{24}H_{21}FN_2O_4S.3/2\,H_2O$: C, 60.11; H, 5.04; N, 5.84; S, 6.69; found: C, 60.46; H, 4.58; N, 5.81; S, 6.47%.

N-[2-(3-phenoxyphenyl)-4-oxo-1,3-thiazolidin-3-yl]-2-(3-methylphenoxy)acetamide (4d). Off-white solid; yield: 69%; mp 149–150 °C; FTIR (v, cm^{-1}) = 3211 (N-H), 1714 & 1681 (C = O); ^{1}H-NMR (300 MHz), (DMSO-d_6/TMS) δ ppm: 2.24 (s, 3H, Ar-C**H**$_3$), 3.72-3.93 (dd, 2H, J = 15.6 Hz, thiazolidinone C**H**$_2$ heterocycle), 4.52 (s, 2H, O-C**H**$_2$), 5.81 (s, 1H, S-C**H**-N), 6.62-7.42 (m, 13H, Ar-**H**), 10.53 (s, 1H, CO-N**H**); ^{13}C-NMR ($CDCl_3$, 100 MHz) δ ppm: 21.6 (Ar-**C**H$_3$); 30.0 (thia. **C**$_5$), 62.6 (thia. **C**$_2$), 67.1 (O**C**H$_2$), 157.0 (=**C**H-O-Phenyl), 158.0 (=**C**H-OCH$_2$), 167.2 (amide **C = O**), 169.8 (thia. C = O); Anal. Calcd. for $C_{24}H_{22}N_2O_4S.H_2O$: C, 63.70; H, 5.35; N, 6.19; S, 7.09; found: C, 63.65; H, 4.97; N, 6.09; S, 7.04%.

N-[2-(4-phenylthiophen-2-yl)-4-oxo-1,3-thiazolidin-3-yl]-2-(3-methylphenoxy)acetamide (4e). Pale yellow solid; yield: 50%; mp 124–126 °C; FTIR (v, cm^{-1}) = 3225 (N-H), 1712 & 1674 (C = O); ^{1}H-NMR (300 MHz), (DMSO-d_6/TMS) δ ppm: 2.21 (s, 3H, Ar-C**H**$_3$), 3.77-3.95 (dd, 2H, J = 15.6 Hz, thiazolidinone C**H**$_2$ heterocycle), 4.58 (s, 2H, O-C**H**$_2$), 6.12 (s, 1H, S-C**H**-N), 6.77-7.96 (m, 11H, Ar-**H**), 10.62 (s, 1H, CO-N**H**); ^{13}C-NMR ($CDCl_3$, 100 MHz) δ ppm: 21.5 (Ar-**C**H$_3$), 30.1 (thia. **C**$_5$), 58.4 (thia. **C**$_2$), 66.9 (O**C**H$_2$), 156.9 (=**C**H-OCH$_2$), 167.4 (amide **C = O**), 169.9 (thia. C = O); Anal. Calcd. for $C_{22}H_{20}N_2O_3S_2.H_2O$: C, 59.71; H, 5.01; N, 6.33; S, 14.49; found: C, 59.73; H, 4.73; N, 6.52; S, 14.82%.

2-(3-Methylphenoxy)-N-{4-oxo-2-[4-(trifluoromethoxy)-phenyl]-1,3-thiazolidin-3-yl}acetamide (4f). White solid; yield: 72%; mp 92 °C; FTIR (v, cm^{-1}) = 3460 (O-H, H_2O), 3239 (N-H), 1714 & 1681 (C = O); ^{1}H-NMR (300 MHz), (DMSO-d_6/TMS) δ ppm: 2.22 (s, 3H, Ar-C**H**$_3$), 3.74-3.97 (dd, 2H, J = 15.9 Hz, thiazolidinone C**H**$_2$ heterocycle), 4.52 (s, 2H, O-C**H**$_2$), 5.86 (s, 1H, S-C**H**-N), 6.59-7.62 (m, 8H, Ar-**H**), 10.49 (s, 1H, CO-N**H**); Anal. Calcd. for $C_{19}H_{17}F_3N_2O_4S.3/4H_2O$: C, 51.87; H, 4.24; N, 6.37; S, 7.29; found: C, 51.68; H, 3.86; N, 6.37; S, 7.29%.

N-[2-(4-fluoro-3-methoxyphenyl)-4-oxo-1,3-thiazolidin-3-yl]-2-(3-methylphenoxy)acetamide (4g). Pale brown solid; yield: 63%; mp 90 °C; FTIR (v, cm^{-1}) = 3261 (N-H), 1716 & 1668 (C = O); ^{1}H-NMR (300 MHz), (DMSO-d_6/TMS) δ ppm: 2.21 (s, 3H, Ar-C**H**$_3$), 3.73-3.93 (m, 5H, thiazolidinone C**H**$_2$ heterocycle & Ar-OC**H**$_3$) , 4.52 (s, 2H, O-C**H**$_2$), 5.84 (s, 1H, S-C**H**-N), 6.59-7.26 (m, 7H, Ar-**H**), 10.46 (s, 1H, CO-N**H**); ^{13}C-NMR ($CDCl_3$, 100 MHz) δ ppm: 21.5 (Ar-**C**H$_3$), 30.2 (thia. **C**$_5$), 56.4 (thia. **C**$_2$), 62.8 (O**C**H$_2$), 67.1 (O**C**H$_3$), 154.3 (=**C**H-OCH$_3$), 156.8 (=**C**H-OCH$_2$), 167.3 (amide **C = O**), 169.7 (thia. C = O); Anal. Calcd. for $C_{19}H_{19}FN_2O_4S.H_2O$: C, 55.87; H, 5.18; N, 6.87; S, 7.85; found: C, 55.51; H, 4.81; N, 6.67; S, 8.08%.

2-(3-Methylphenoxy)-N-{4-oxo-2-[2-(trifluoromethyl)-phenyl]-1,3-thiazolidin-3-yl}acetamide (4h). Pale brown solid; yield: 63%; mp 125–126 °C; FTIR (v, cm^{-1}) = 3236 (N-H), 1714 & 1681 (C = O); ^{1}H-NMR (300 MHz), (DMSO-d_6/TMS) δ ppm: 2.22 (s, 3H, Ar-C**H**$_3$), 3.78–3.97 (dd, 2H, J = 15.6 Hz, thiazolidinone C**H**$_2$ heterocycle), 4.52 (s, 2H, O-C**H**$_2$), 6.06 (s, 1H, S-C**H**-N), 6.61-7.76 (m, 8H, Ar-**H**), 10.58 (s, 1H, CO-N**H**); ^{13}C-NMR ($CDCl_3$, 100 MHz) δ ppm: 21.5 (Ar-**C**H$_3$), 29.8 (thia. **C**$_5$), 56.5 (thia. **C**$_2$), 67.1 (O**C**H$_2$), 156.8 (=**C**H-OCH$_2$), 167.2 (amide **C = O**), 169.7 (thia. C = O); Anal. Calcd. for

Table 3. *In silico* ADMET prediction of the selected compounds.

Property	Predicted value					
	3h	3i	4a	4d	4h	4i
Absorption						
Water solubility (log mol/L)	−5.208	−5.121	−5.165	−6.510	−5.551	−5.647
Caco-2 permeability (log Papp in 10^{-6} cm/s)	1.379	1.398	1.101	1.078	1.084	1.349
Intestinal absorption (human) (% absorbed)	90.759	90.936	93.677	93.157	90.604	92.041
Skin permeability (log Kp)	−2.804	−2.771	−3.371	−2.77	−3.156	−3.323
Distribution						
BBB permeability (log BB)	0.21	0.259	−0.558	−0.341	−0.776	−0.178
Metabolism categorical (yes/no)						
CYP2D6 substrate	No	No	No	No	No	No
CYP3A4 substrate	Yes	Yes	Yes	Yes	Yes	Yes
CYP1A2 inhibitor	Yes	Yes	No	No	No	No
CYP2C19 inhibitor	Yes	Yes	Yes	Yes	Yes	Yes
CYP2C9 inhibitor	No	No	Yes	Yes	Yes	Yes
CYP2D6 inhibitor	No	No	No	No	No	No
CYP3A4 inhibitor	No	No	Yes	Yes	Yes	Yes
Excretion						
Total clearance (log mL/min/kg)	0.261	−0.197	0.194	−0.193	0.031	−0.219
Toxicity categorical (yes/no)						
AMES toxicity	No	No	No	No	No	No
Hepatotoxicity	No	No	No	No	Yes	No
Skin sensitisation	No	No	No	No	No	No

AMES: assay of the ability of a chemical compound to induce mutations in DNA; BBB: blood–brain barrier (log BB > 0.3 (cross BBB), log BB < −1 (poorly distributed brain); (http://biosig.unimelb.edu.au/pkcsm/prediction).

$C_{19}H_{17}F_3N_2O_3S.6H_2O$: C, 44.10; H, 5.64; N, 5.40; S, 6.18; found: C, 44.24; H, 5.43; N, 5.44; S, 6.28%.

N-[2-(3,5-dichlorophenyl)-4-oxo-1,3-thiazolidin-3-yl]-2-(3-methylphenoxy)acetamide (4i). White solid; yield: 78%; mp 144–146 °C; FTIR (v, cm^{-1}) = 3188 (N-H), 1714 & 1660 (C = O); ^{1}H-NMR (300 MHz), (DMSO-d_6/TMS) δ ppm: 2.24 (s, 3H, Ar-C**H**$_3$), 3.72-4.04 (dd, 2H, J = 15.6 Hz, thiazolidinone C**H**$_2$ heterocycle), 4.55 (s, 2H, O-C**H**$_2$), 5.82 (s, 1H, S-C**H**-N), 6.62-7.60 (m, 7H, Ar-**H**), 10.57 (s, 1H, CO-N**H**); ^{13}C-NMR ($CDCl_3$, 100 MHz) δ ppm: 21.6 (Ar-**C**H$_3$), 30.0 (thia. **C**$_5$), 61.9 (thia. **C**$_2$), 66.9 (O**C**H$_2$), 156.9 (=**C**H-OCH$_2$), 167.5 (amide **C = O**), 169.8 (thia. C = O); Anal. Calcd. for $C_{18}H_{16}Cl_2N_2O_3S$: C, 52.56; H, 3.92; N, 6.81; S, 7.80; found: C, 52.11; H, 3.53; N, 7.01; S, 8.38%.

N-[2-(3,4-dimethylphenyl)-4-oxo-1,3-thiazolidin-3-yl]-2-(3-methylphenoxy)acetamide (4j). Off-white solid; yield: 58%; mp 149–150 °C; FTIR (v, cm^{-1}) = 3182 (N-H), 1714 & 1668 (C = O); ^{1}H-NMR (300 MHz), (DMSO-d_6/TMS) δ ppm: 2.25 (s, 3H, Ar-C**H**$_3$), 2.27 (s, 3H, Ar-C**H**$_3$), 2.28 (s, 3H, Ar-C**H**$_3$), 3.06-3.87 (m, 2H, thiazolidinone C**H**$_2$ heterocycle), 4.62 & 5.10 (2 s, 2H, O-C**H**$_2$), 6.81-8.25 (m, 8H, Ar-**H &** S-C**H**-N), 11.48 & 11.51 (2s, 1H, CO-N**H**); Anal. Calcd. for $C_{20}H_{22}N_2O_3S$: C, 64.84; H, 5.99; N, 7.56; S, 8.66; found: C, 64.64; H, 5.82; N, 8.45; S, 8.80%.

2.2. Microdilution test for antimicrobial activity

After synthesis and purification, we tested the antimicrobial activities of the compounds against the American Type Culture Collection® (ATCC) strains of *Escherichia coli* (ATCC 25922), *Staphylococcus aureus* (ATCC 29213), *Enterococcus faecalis* (ATCC 29212), *Pseudomonas aeruginosa* (ATCC 27853) and *Candida krusei* (ATCC 6258), *Candida albicans* (ATCC 90028) and *Candida parapsilosis* (ATCC 90018) by broth microdilution method in accordance with the Clinical and Laboratory Standards Institute (CLSI) reference documents (CLSI, 2008; CLSI, 2018). Ciprofloxacin and Fluconazole were used as reference drugs.

The fungal and bacterial isolates were subcultured onto Sabouraud dextrose agar and Mueller Hinton agar, respectively prior to testing. For fungi, broth microdilution was performed using RPMI 1640 broth (ICN-Flow, with glutamine, without bicarbonate and with pH indicator) buffered to pH 7.0 with 3-*N*-morpholinopropanesulfonic acid (MOPS). For bacteria, microdilution test was conducted using Mueller Hinton broth (MHB, Difco Laboratories, USA) buffered to pH 7.0 with 3-*N*-morpholinopropanesulfonic acid (MOPS, Sigma, USA). The final test concentration of fungi and bacteria was 0.5 to 2.5×10^3 cfu/mL and 5×10^5 cfu/mL, respectively. After dissolving the compounds in DMSO, their final two fold concentrations (1024 to 1 μg/mL) were prepared in the wells of the microtiter plates. The plates for bacteria and fungi were incubated at 35 °C for 18–24 h and 48 h, respectively. MIC values were read as the lowest concentration (μg/mL) of test compound that fully inhibited visual microorganism growth.

2.3. Molecular modeling studies

2.3.1. Drug likeness and ADMET analysis

The chemical structures of the selected molecules were sketched, SMILES codes were generated, and the descriptors indicating the compounds' drug-likeness were computed in SwissADME (Daina et al., 2017). ADMET properties such as water solubility, Caco-2 permeability, intestinal absorption, blood brain barrier (BBB) permeability along with metabolism and toxicity parameters were predicted using pkCSM web server (Pires et al., 2015).

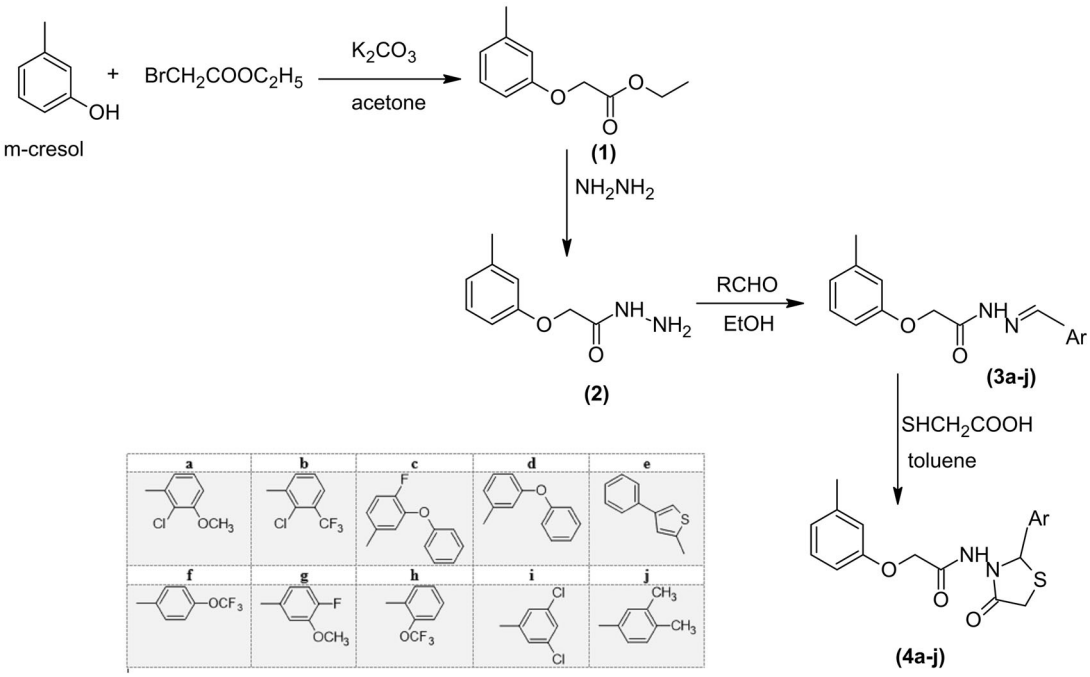

Scheme 1. Syntetic route of m-cresol derivatives (**3a-j** and **4a-j**).

2.3.2. Molecular docking

The crystal structure of pyruvate dehydrogenase multienzyme complex E1 component (PDHc-E1) from *E. coli* was obtained from Protein Data Bank (PDB ID: 1L8A, Resolution: 1.85 Å) (Arjunan et al., 2002). The chemical structures of **3h**, **4d**, and m-cresol were sketched and energy minimized using the MMFF94 force field in LigandScout 4.4 (Wolber & Langer, 2005). The compounds were subsequently docked into the binding site of the cofactor thiamin diphosphate (ThDP) using AutoDock 4.2 (Morris et al., 2009), implemented in LigandScout, with default parameters. The most plausible binding modes were selected upon the visual analysis of the obtained docking poses in LigandScout. 3D and 2D representations of the interactions were prepared using Maestro (Schrödinger Release 2019-1: Maestro, 2019).

3. Results and discussion

3.1. Chemistry

The title products **3a-j** and **4a-j** were synthesized using the reactions depicted in Scheme 1. Compounds **1** and **2** were obtained by previously described procedures (Kulabaş et al., 2016; Şenkardeş et al., 2021). Condensation of **2** with the various aldehydes in ethanol yielded the hydrazide-hydrazones **3a-j**. The reaction of **3a-j** with thioglycolic acid in toluene yielded 4-thiazolidinones. Among the newly synthesized compounds, compounds **3d** and **3 g** have got only CAS numbers (CAS No: 351871-47-1 and 2486106-08-3, respectively) with no spectroscopic data. So, all newly synthesized compounds were checked for purity using elemental microanalysis and fully characterized by their spectral data and melting points.

The structures of the molecules were confirmed by elemental analysis, FTIR spectra and NMR analyses. In the IR spectra of **3a-j**, C = O bands were observed in the 1674–1680 cm^{-1} regions. The IR spectra of **4a-j** exhibited another C = O band (1712–1716 cm^{-1}) which indicated the presence of a thiazolidinone ring.

According to literature, the hydrazone moieties may present as E/Z isomers about C = N bonds and cis/trans CO-NH conformers. Literature survey reveals that both cis and trans conformers are observed in polar aprotic solvents (Koç et al., 2022; Palla et al., 1986). When we analyse ^{1}H-NMR spectra of hydrazone derivatives in DMSO-d_6 as an aprotic solvent; we observed two singlets for each of the methylene, azomethine and amide protons corresponding to E and Z forms. As indicated in our previous article (Şenkardeş et al., 2021), aromatic methyl protons of **3a-j** appeared at 2.25-2.29 ppm as a double singlet. The disappearance of the azomethine signal and the appearance of a signal for the thiazolidinone ring CH displayed the ring closure. Multiplets or double doublet peaks at δ values between 3.52 and 4.04 ppm suggest the presence of CH_2 protons of the ring in the **4a-j** derivatives. Finally, peaks for phenyl and thienyl protons in the compounds appeared between 6.59–8.33 ppm.

3.2. Biological evaluation

Antibacterial and antifungal activities of the compounds **3a-j** and **4a-j** were tested using microbroth dilution method. Tested organism strains were; *S. aureus* (ATCC 29213), *P. aeruginosa* (ATCC 27853), *E. faecalis* (ATCC 29212), and *E. coli* (ATCC 25922) as bacteria and *C. albicans* (ATCC 90028), *C. parapsilosis* (ATCC 90018) and *C. krusei* (ATCC 6258) as fungal strains. The observed data on the activity of the products are shown in Table 1.

P. aeruginosa causes severe acute and chronic infections in the host body, including the skin, urinary tract, and respiratory system (Mansuri et al., 2022). Compounds **3b**, **3i**

Table 1. Antimicrobial activities of the compounds **3a-j** and **4a-j**.

	Minimum Inhibitory Concentration (μg ml^{-1})						
Comp.	*S. aureus*	*E. faecalis*	*P. aeruginosa*	*E. coli*	*C. albicans*	*C. parapsilosis*	*C. krusei*
3a	256	256	256	128	128	256	128
3b	256	64	16	16	64	256	256
3c	128	128	64	32	128	64	64
3d	128	64	128	16	256	64	128
3e	256	32	512	32	256	256	512
3f	128	64	32	64	128	256	1024
3g	64	256	512	256	512	256	512
3h	256	256	128	4	128	64	128
3i	32	64	16	8	32	32	16
3j	512	2048	1024	256	512	512	1024
4a	64	256	128	4	256	256	128
4b	64	128	128	8	256	128	64
4c	256	128	64	64	64	128	1024
4d	512	256	64	2	128	256	1024
4e	64	128	64	32	64	128	64
4f	128	64	32	32	128	64	32
4g	128	128	128	32	128	128	64
4h	32	32	16	4	64	64	1024
4i	8	64	128	2	256	128	64
4j	64	64	64	16	128	128	64
CIP	0.125	0.5	0.125	0.0625	–	–	–
FLU	–	–	–	–	1	1	16

CIP: ciprofloxacin,FLU: fluconazole.

Table 2. Predicted drug-likeness parameters of the selected compounds.

Compound	M.W.	Log*P*	HBD	HBA	Lipinski's Violation	NROTB	TPSA
3h	352.31	3.77	1	7	0	8	59.92
3i	337.20	3.88	1	3	0	6	50.69
4a	406.88	3.03	1	4	0	7	93.17
4d	434.51	3.76	1	4	0	8	93.17
4h	410.41	3.57	1	6	0	7	83.94
4i	411.30	3.53	1	3	0	6	83.94

M.W: molecular weight, Log*P*: logarithm of n-octanol-water partition coefficient, HBD: number of hydrogen bond donors, HBA: number of hydrogen bond acceptors, NROTB: number of rotatable bonds, TPSA: topological polar surface area.

and **4h** have shown same potency (MIC= 16 μg/mL) against *P. aeruginosa*. Furthermore, compounds **3h**, **3i**, **4a**, **4b**, **4d**, **4h** and **4i** showed low MICs in the range of 2–8 μg/mL against *E. coli*. Compound **4i** with 3,5-dichlorophenyl substituent also showed the highest effect against *S. aureus*, which represents Gram positive bacteria with MIC of 8 μg/mL. This study showed that these m-cresol derivatives were particularly effective against *E. coli*.

On the other hand, from the data shown in Table 1, it is clear that *N*′-[(3,5-dichlorophenyl)methylidene]-2-(3-methylphenoxy)acetohydrazide **(3i)** exhibited the lowest MIC values in the range of 16–32 μg/mL against pathogenic fungal strains, particularly as effective as standard Fluconazole (MIC value= 16 μg/mL) against *C. krusei*. These data clearly demonstrated that the 3,5-dichlorophenyl substituent plays a major role in antimicrobial activity of these derivatives.

3.3. In silico studies

3.3.1. In silico prediction of drug-likeness and ADMET profiles

When turning bioactive compounds into drug molecules, unsuitable physicochemical properties can stand as a significant impediment. Hence, we computed drug-likeness parameters of the selected compounds. We picked up the molecules exhibiting antibacterial activity against *E. coli* with MIC value ≤4 μg/mL (**3h**, **4a**, **4d**, **4h**, and **4i**) and also **3i** as the most active antifungal derivative. Initially, we calculated the physicochemical properties constituting Lipinski's rule-of-five. This rule of thumb states that an orally active drug should not break more than one of these criteria: molecular weight less than 500 Da, the octanol–water partition coefficient (Log *P*) not greater than 5, no more than 5 hydrogen bond donors, and no more than 10 hydrogen bond acceptors (Lipinski et al., 2001). Furthermore, we computed topological polar surface area and the number of rotatable bonds which are also considered critical parameters for the oral bioavailability prediction of novel compounds (Veber et al., 2002). The calculated parameters of the most active molecules are reported in Table 2.

Based on these results, all selected compounds adhered to Lipinski's rules. Among them, lipophilicity is particularly regarded as an important parameter for drug design and development process (Arnott & Planey, 2012). This molecular descriptor plays a central role not only in the transport of drugs through biological systems but also in the interactions of drugs with their biological targets (Testa et al., 2000). Lipophilicity is considered one of the main structural properties of antimicrobial agents correlating with their biological effects (Testa et al., 2000; Ullah et al., 2018). Therefore, one of the factors determining the antimicrobial activity of the selected compounds is likely to be their lipophilic characters. Rotatable bonds count is a considerable parameter indicating the number of bonds that rotate freely around themselves and should be <10. Our selected compounds obeyed this rule with ≤10 rotatable bonds. Since most therapeutics have topological polar surface area less than 140–150 Å^2, our compounds also stay in the favorable range with their values varying from 50.69 to 93.17 Å^2 (Ertl et al., 2000).

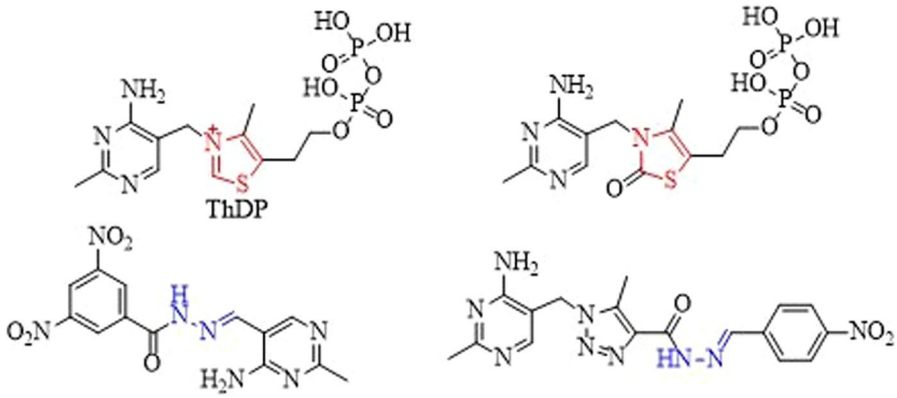

Figure 3. Chemical structures of ThDP and some recently reported PDHc-E1 inhibitors with thiazole or hydrazone moieties.

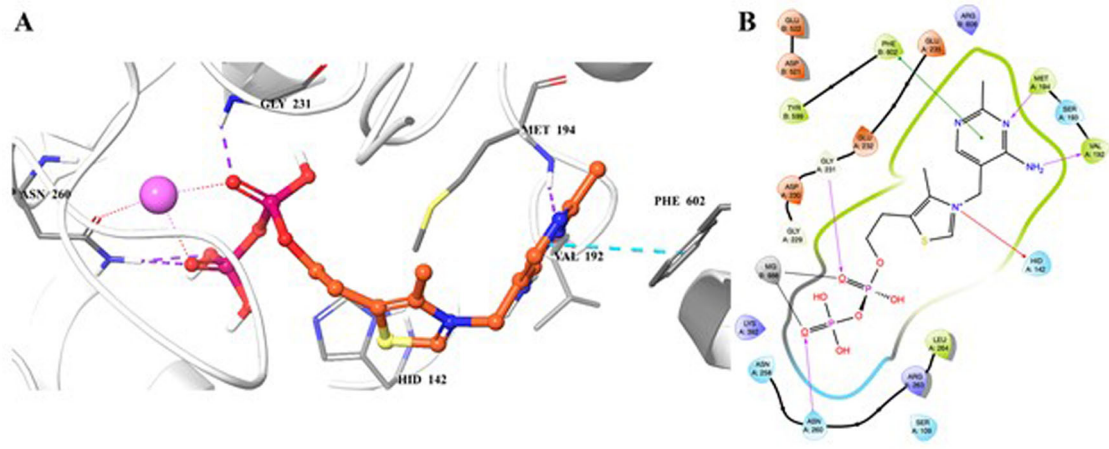

Figure 4. Binding mode of thiamine diphosphate (ThDP) (A) and 2 D depiction of ligand-enzyme interactions (B) in the cofactor binding pocket of *E. coli* PDHc-E1 (PDB Code:1L8A). ThDP is represented as orange stick and balls, amino acid residues as gray sticks, protein backbone as white cartoons, binding interactions as color dashes (purple for hydrogen bond, cyan for π-π), and the magnesium ion as faded pink sphere.

Organic molecules' solubility is another important parameter. Poor aqueous solubility of drug candidates is one of the most significant barriers to drug discovery. From the pkCSM results shown in Table 3, it was observed that the compounds tested are moderately soluble. (Insoluble $\leq$ −10 poorly soluble $<$ −6 $<$ moderately $<$ −4 $<$ soluble $<$ −2 very soluble $<$ 0 $\leq$ highly soluble) (Amin et al., 2022).

The predictive model of pkCSM shows that these molecules with predicted values $>$0.9 have high Caco2 cell permeability. According to Chander et al. (2017), a compound is considered to have good absorption if its absorption value is greater than 80%, and it is considered to have poor absorption if it is less than 30%. Table 3 shows that the six compounds have good absorption. These derivatives have log values of K_p $<$−2.5, meaning that these compounds have good permeability on the skin (Pires et al., 2015). Also, these compounds cannot penetrate the blood-brain barrier because they do not have log BB values of $>$0.3 (Pires et al., 2015).

The cytochrome P450 (CYP) family catalyzes drug metabolism and thus is relevant to drug development. The subtype of cytochrome P450 CYP2D6 shows that compounds could not be substrates or inhibitors of this main subtype, which can reduce the possibility of drug-drug interactions. According to data, compounds **4a**, **4d**, **4h** and **4i** are CYP2C9 and CYP3A4 inhibitors, while CYP1A2 was not inhibited by these compounds *in silico*. Additionally, all the studied compounds were found to be a substrate of CYP3A4 and an inhibitor of CYP2C19.

To predict the compounds' excretion process, the total clearance, a combination of hepatic clearance and renal clearance, was calculated. A drug with a high total clearance value will be excreted quickly. Compounds present total clearance values ranging from −0.219 to 0.261. Also, they present no AMES toxicity and skin sensibilization, only compound **4h** can be hepatotoxic.

Consequently, the studied molecules possess suitable physicochemical and ADMET properties that make them antimicrobial drug candidates.

3.3.2. Molecular docking

The synthesized compounds were particularly effective against *E. coli*. Therefore, we aimed to rationalize the obtained biological data and find out the potential antibacterial activity mechanism through molecular docking studies.

The pyruvate dehydrogenase complex (PDHc) consisting of three enzymes catalyzes the conversion of pyruvate into acetyl coenzyme A (acetyl-CoA) initiated by the oxidative decarboxylation of pyruvate. Due to this function, PDHc plays a central role in the cellular metabolism of organisms (Patel & Korotchkina, 2003).

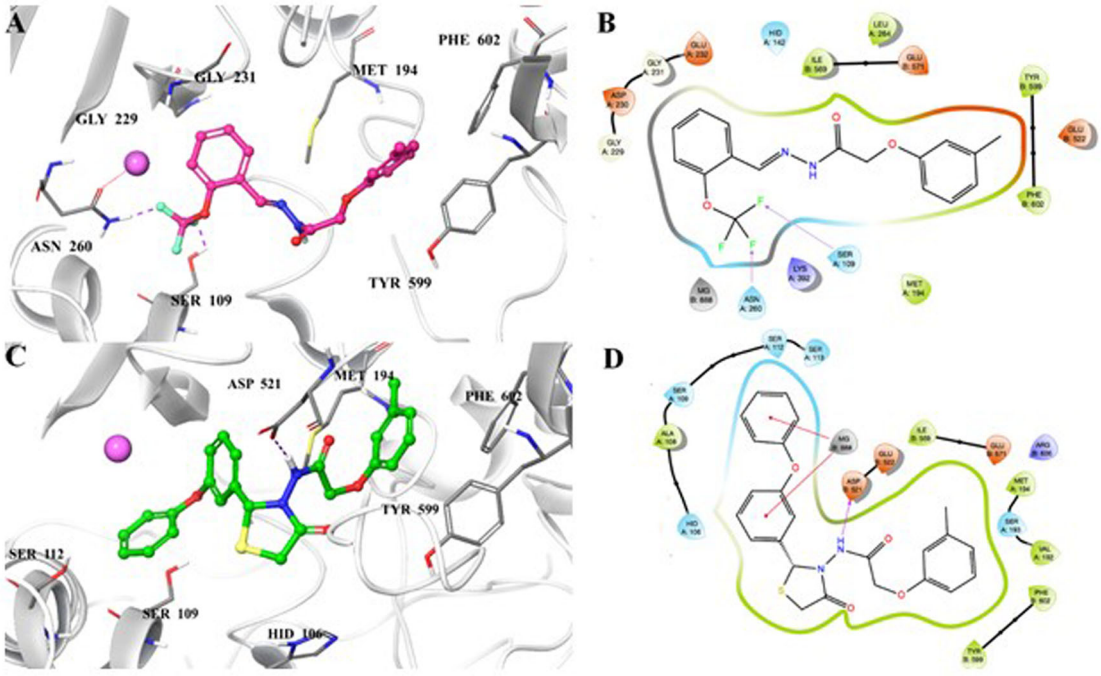

Figure 5. Three-dimensional interactions of **3h** (A) and **4d** (C) in the ThDP binding site of *E. coli* PDHc-E1. 2D ligand-enzyme interactions are represented for **3h** (B) and **4d** (D). Ligands are shown as pink (**3h**) and green (**4d**) balls and sticks, some key amino acid residues participating in ligand binding as gray sticks, protein backbone as white cartoon, hydrogen bonds as purple dashes, and the magnesium ion as faded pink sphere.

The first member of this complex is pyruvate dehydrogenase (E1) which is responsible for the initial step of this multistep process employing thiamine diphosphate (ThDP) and magnesium ion (Mg^{2+}) as cofactors (Patel et al., 2014). Hence, inhibiting PDHc-E1 is considered an effective strategy to block PDHc activity. As ThDP is one of the essential cofactors that regulate PDHc-E1 activity, blocking its active site with an inhibitor is a rational approach to inactivate the enzyme.

The researchers gave much effort to design and synthesize new PDHc-E1 inhibitors. ThDP analogs carrying core thiazole-based moieties were often developed to target the binding site of ThDP. Despite their high binding affinities, they exhibited low bioavailability and no potential utility because of their highly charged phosphate groups (Arjunan et al., 2006; Nemeria et al., 2001). Subsequently, other chemical groups of compounds were considered to block PDHc-E1 activity. Among them, hydrazone functionality was one of the most common pharmacophores present in the structures of newly designed inhibitors (Figure 3) (He et al., 2017; Zhou et al., 2021).

Prompted by these considerations and the pharmacophore similarity of our compounds with the previously reported inhibitors, we aimed to support the high antibacterial activity against *E. coli* by molecular docking studies into the cofactor (ThDP) binding site of *E. coli* PDHc-E1. We picked up the most active compound from each series: **3h** from hydrazone derivatives and **4d** from thiazolidinones. We additionally docked m-cresol to determine how the modifications on this core moiety affect the activities of our compounds on *E. coli* PDHc-E1.

We initially examined the interactions of thiamine diphosphate (ThDP) within the cofactor binding site of *E. coli* PDHc-E1 (Figure 4).

Diphosphate group of ThDP interacts with the enzyme in two ways; through forming hydrogen bonds to Gly231 and Asn260, and through interacting with Mg^{2+} ion. Furthermore, ThDP adopts a "V" conformation allowing thiazolium ring mainly interact with Hid142. Aminopyrimidine moiety participates in binding to the active site of *E. coli* PDHc-E1 through hydrogen bonds with Val192 and Val194. π-π stacking between aminopyrimidine ring and Phe602 is also observed.

Subsequently, we compared the binding interactions of **3h** and **4d** in the ThDP binding site of *E. coli* PDHc-E1 with the co-crystallized ligand ThDP.

Based on the obtained interactions shown in Figure 5, **3h** occupied ThDP binding site in a "V" conformation similar to ThDP with the estimated binding energy of –10.42 kcal/mol. 3-Methylphenyl ring was responsible for hydrophobic contacts, particularly to Tyr599, Phe602, and Met194. On the other side of the molecule, 2-(trifluoromethoxy)phenyl moiety formed additional hydrophobic interactions. 2-OCF_3 substituent on this phenyl ring oriented towards the Mg ion and formed two key hydrogen bonds to Ser109 and Asn260, in the same way as ThDP. The low MIC value of **3h** against *E. coli* can be explained due to the similar binding mode of **3 h** to ThDP. When the interactions of **4d** in the same binding site (binding energy: –8.86 kcal/mol) were examined, it was observed that 3-methylphenoxy moiety occupied the same lipophilic pocket providing hydrophobic interactions with the enzyme. N-H group of acetamide functionality formed a hydrogen bond to Asp521 to stabilize the ligand in the active pocket. It is noteworthy that two phenyl rings on the other side of the molecule formed π-cation interactions with Mg^{2+}, the other co-factor of the enzyme.

We also docked our starting compound m-cresol in the same binding pocket. Due to its less bulky structure compared to our final compounds, m-cresol could only occupy the phosphate binding site of the pocket. Therefore, as expected, its estimated binding energy is higher (–4.70 kcal/mol) than our final compounds. This situation shows that the modifications on m-cresol leading to hydrazone or thiazolidine-4-one moieties are beneficial to the binding of the studied molecules to the cofactor (ThDP) binding site of *E. coli* PDHc-E1.

As a result, molecular docking studies point out the inhibition of the cofactor binding site of PDHc-E1 as the potential antibacterial mechanism of our compounds against *E. coli*. It is also highlighted that the substituent type on the phenyl ring is significant for the antibacterial activity trend of these molecules against *E. coli*.

4. Conclusion

The hydrazones and 4-thiazolidinones of m-cresol were readily prepared for evaluation of their antimicrobial activity. According to the activity results, some of the synthesized compounds demonstrated remarkable antibacterial effects on *E. coli* that causes serious infections by consuming contaminated food and water or by contacting infected people. Among them, compounds **4d** and **4i** were the most promising derivatives against *E. coli* with MIC value of 2 μg/mL. Additionally, compound **3i** exhibited comparable antifungal activity to fluconazole against *Candida krusei* is well known as a fungal nosocomial pathogen. Calculated physicochemical descriptors of the most active compounds demonstrated that they can be considered drug candidates. The inhibition of the cofactor binding site of *E. coli* PDHc-E1 was determined as the potential activity mechanism of the compounds against *E. coli* through molecular docking studies. Altogether, our results may be useful for further improvements in development of new antimicrobial drugs.

Acknowledgements

We thank Dr. Esen Bellur Atıcı from Deva Holding A.Ş. (Turkey), for her generous help on obtaining ^{13}C-NMR spectra of the synthesized compounds. MGG also would like to thank Prof. Dr. Gerhard Wolber (Freie Universität Berlin) for supplying the LigandScout 4.4. license.

Disclosure statement

No potential conflict of interest was reported by the authors

Funding

The author(s) reported there is no funding associated with the work featured in this article.

ORCID

Sevil Şenkardeş http://orcid.org/0000-0002-0523-459X
Miyase Gözde Gündüz http://orcid.org/0000-0002-2287-9509
Ş Güniz Küçükgüzel http://orcid.org/0000-0001-9405-8905

Data availability statement

The data that supports the findings of this work are available in the supplementary material.

References

Amin, M., Yasmin, F., Dey, S., Dey, S., Mahmud, S., Saleh, M. A., Emran, T. B., Hasan, I., Rajia, S., Ogawa, Y., Fujii, Y., Yamada, M., Ozeki, Y., & Kawsar, S. M. A. (2022). Methyl β-D-galactopyranoside esters as potential inhibitors for SARS-CoV-2 protease enzyme: Synthesis, antimicrobial, PASS, molecular docking, molecular dynamics simulations and quantum computations. *Glycoconjugate Journal*, *39*(2), 261–290. https://doi.org/10.1007/s10719-021-10039-3

Arjunan, P., Nemeria, N., Brunskill, A., Chandrasekhar, K., Sax, M., Yan, Y., Jordan, F., Guest, J. R., & Furey, W. (2002). Structure of the pyruvate dehydrogenase multienzyme complex E1 component from *Escherichia coli* at 1.85 Å resolution. *Biochemistry*, *41*(16), 5213–5221. https://doi.org/10.1021/BI0118557

Arjunan, P., Sax, M., Brunskill, A., Chandrasekhar, K., Nemeria, N., Zhang, S., Jordan, F., & Furey, W. (2006). A thiamin-bound, pre-decarboxylation reaction intermediate analogue in the pyruvate dehydrogenase E1 subunit induces large scale disorder-to-order transformations in the enzyme and reveals novel structural features in the covalently bound adduct. *The Journal of Biological Chemistry*, *281*(22), 15296–15303. https://doi.org/10.1074/JBC.M600656200

Arnott, J. A., & Planey, S. L. (2012). The influence of lipophilicity in drug discovery and design. *Expert Opinion on Drug Discovery*, *7*(10), 863–875. https://doi.org/10.1517/17460441.2012.714363

Chander, S., Tang, C. R., Al-Maqtari, H. M., Jamalis, J., Penta, A., Hadda, T. B., Sirat, H. M., Zheng, Y. T., & Sankaranarayanan, M. (2017). Synthesis and study of anti-HIV-1 RT activity of 5-benzoyl-4-methyl-1,3,4,5-tetrahydro-2H-1,5-benzodiazepin-2-one derivatives. *Bioorganic Chemistry*, *72*, 74–79. https://doi.org/10.1016/j.bioorg.2017.03.013

Cikla, P., Tatar, E., Küçükgüzel, I., Şahin, F., Yurdakul, D., Basu, A., Krishnan, R., Nichols, D. B., Kaushik-Basu, N., & Küçükgüzel, Ş. G. (2013). Synthesis and characterization of flurbiprofen hydrazide derivatives as potential anti-HCV, anticancer and antimicrobial agents. *Medicinal Chemistry Research*, *22*(12), 5685–5699. https://doi.org/10.1007/s00044-013-0550-3

Clinical and Laboratory Standards Institute (CLSI). (2008) Reference method for broth dilution antifungal susceptibility testing of yeasts; approved standard. In: *M27-A3* (3rd ed., Replaces M27-A2). Clinical and Laboratory Standards Institute.

Daina, A., Michielin, O., & Zoete, V. (2017). SwissADME: A free web tool to evaluate pharmacokinetics, drug-likeness and medicinal chemistry friendliness of small molecules. *Scientific Reports*, *7*(January), 42717–42713. https://doi.org/10.1038/srep42717

Datar, P. A., & Aher, S. B. (2016). Design and synthesis of novel thiazolidine-2,4-diones as hypoglycemic agents. *Journal of Saudi Chemical Society*, *20*, S196–S201. https://doi.org/10.1016/j.jscs.2012.10.010

de la Fuente-Nunez, C., Torres, M. D., Mojica, F. J., & Lu, T. K. (2017). Next-generation precision antimicrobials: towards personalized treatment of infectious diseases. *Current Opinion in Microbiology*, *37*, 95–102. https://doi.org/10.1016/j.mib.2017.05.014

Del Carmen Cruz, M., Salazar, M., Garciafigueroa, Y., Hernández, D., Díaz, F., Chamorro, G., & Tamariz, J. (2003). Hypolipidemic activity of new phenoxyacetic derivatives related to α-asarone with minimal pharmacophore features. *Drug Development Research*, *60*(3), 186–195. https://doi.org/10.1002/ddr.10281

Ertl, P., Rohde, B., & Selzer, P. (2000). Fast calculation of molecular polar surface area as a sum of fragment-based contributions and its application to the prediction of drug transport properties. *Journal of Medicinal Chemistry*, *43*(20), 3714–3717. https://doi.org/10.1021/jm000942e

Gajdács, M., & Albericio, F. (2019). Antibiotic resistance: from the bench to patients. *Antibiotics*, *8*(3), 129–111. https://doi.org/10.3390/antibiotics8030129

Han, M. İ., Atalay, P., Tunç, C. Ü., Ünal, G., Dayan, S., Aydı n, Ö., & Küçükgüzel, ŞG. (2021). Design and synthesis of novel (S)-Naproxen hydrazide-hydrazones as potent VEGFR-2 inhibitors and their evaluation in vitro/in vivo breast cancer models. *Bioorganic & Medicinal Chemistry*, *37*, 116097. https://doi.org/10.1016/j.bmc.2021.116097

He, H., Xia, H., Xia, Q., Ren, Y., & He, H. (2017). Design and optimization of N-acylhydrazone pyrimidine derivatives as *E. coli* PDHc E1 inhibitors: Structure-activity relationship analysis, biological evaluation and molecular docking study. *Bioorganic & Medicinal Chemistry*, *25*(20), 5652–5661. https://doi.org/10.1016/J.BMC.2017.08.038

Jampilek, J. (2019). Heterocycles in medicinal chemistry. *Molecules*, *24*(21), 3839–3813. https://doi.org/10.3390/molecules24213839

Kaushik-Basu, N., Bopda-Waffo, A., Talele, T. T., Basu, A., Chen, Y., & Kucukguzel, S. G. (2008). 4-Thiazolidinones: A novel class of hepatitis C virus NS5B polymerase inhibitors. *Frontiers in Bioscience : A Journal and Virtual Library*, *13*, 3857–3868. https://doi.org/10.2741/2974

Koç, H. C., Atlihan, İ., Mega-Tiber, P., Orun, O., & Küçükgüzel, G. (2022). Synthesis of some novel hydrazide-hydrazones derived from etodolac as potential anti-prostate cancer agents. *Journal of Research in Pharmacy*, *26*(1), 1018–1029. https://doi.org/10.29228/jrp.97

Küçükgüzel, G., Kocatepe, A., De Clercq, E., Sahin, F., & Güllüce, M. (2006). Synthesis and biological activity of 4-thiazolidinones, thiosemicarbazides derived from diflunisal hydrazide. *European Journal of Medicinal Chemistry*, *41*(3), 353–359. https://doi.org/10.1016/j.ejmech.2005.11.005

Küçükgüzel, Ş. G., Mazi, A., Sahin, F., Öztürk, S., & Stables, J. (2003). Synthesis and biological activities of diflunisal hydrazide-hydrazones. *European Journal of Medicinal Chemistry*, *38*(11–12), 1005–1013. https://doi.org/10.1016/j.ejmech.2003.08.004

Küçükgüzel, S. G., Oruç, E. E., Rollas, S., Sahin, F., & Ozbek, A. (2002). Synthesis, characterisation and biological activity of novel 4-thiazolidinones, 1,3,4-oxadiazoles and some related compounds. *European Journal of Medicinal Chemistry*, *37*(3), 197–206. https://doi.org/10.1016/S0223-5234(01)01326-5

Kulabaş, N., Tatar, E., Bingöl Özakpınar, Ö., Özsavcı, D., Pannecouque, C., De Clercq, E., & Küçükgüzel, İ. (2016). Synthesis and antiproliferative evaluation of novel 2-(4H-1,2,4-triazole-3-ylthio)acetamide derivatives as inducers of apoptosis in cancer cells. *European Journal of Medicinal Chemistry*, *121*, 58–70. https://doi.org/10.1016/j.ejmech.2016.05.017

Laxminarayan, R., Duse, A., Wattal, C., Zaidi, A. K. M., Wertheim, H. F. L., Sumpradit, N., Vlieghe, E., Hara, G. L., Gould, I. M., Goossens, H., Greko, C., So, A. D., Bigdeli, M., Tomson, G., Woodhouse, W., Ombaka, E., Peralta, A. Q., Qamar, F. N., Mir, F., … Cars, O. (2013). Antibiotic resistance-the need for global solutions. *The Lancet. Infectious Diseases*, *13*(12), 1057–1098. https://doi.org/10.1016/S1473-3099(13)70318-9

Laxminarayan, R., Matsoso, P., Pant, S., Brower, C., Røttingen, J. A., Klugman, K., & Davies, S. (2016). Access to effective antimicrobials: A worldwide challenge. *The Lancet*, *387*(10014), 168–175. https://doi.org/10.1016/S0140-6736(15)00474-2

Lipinski, C. A., Lombardo, F., Dominy, B. W., & Feeney, P. J. (2001). Experimental and computational approaches to estimate solubility and permeability in drug discovery and development settings. *Advanced Drug Delivery Reviews*, *46*(1-3), 3–26. https://doi.org/10.1016/S0169-409X(00)00129-0

Mansuri, A., Lokhande, K., Kore, S., Gaikwad, S., Nawani, N. K., Swamy, V., Junnarkar, M., & Pawar, S. (2022). Antioxidant, anti-quorum sensing, biofilm inhibitory activities and chemical composition of Patchouli essential oil: in vitro and in silico approach. *Journal of Biomolecular Structure & Dynamics*, *40*(1), 154–165. https://doi.org/10.1080/07391102.2020.1810124

Clinical and Laboratory Standards Institute. (2018). Methods for dilution antimicrobial susceptibility tests for bacteria that grow aerobically (M07, 11th ed., Replaces M07-A10). Clinical and Laboratory Standards Institute.

McCarthy, S. D., Horgan, E., Ali, A., Masterson, C., Laffey, J. G., MacLoughlin, R., & O'Toole, D. (2020). Nebulized mesenchymal stem cell derived conditioned medium retains antibacterial properties against clinical pathogen isolates. *Journal of Aerosol Medicine and Pulmonary Drug Delivery*, *33*(3), 140–152. https://doi.org/10.1089/jamp.2019.1542

Morris, G. M., Huey, R., Lindstrom, W., Sanner, M. F., Belew, R. K., Goodsell, D. S., & Olson, A. J. (2009). AutoDock4 and AutoDockTools4: Automated docking with selective receptor flexibility. *Journal of Computational Chemistry*, *30*(16), 2785–2791. https://doi.org/10.1002/jcc.21256

Murray, C. J., Ikuta, K. S., Sharara, F., Swetschinski, L., Robles Aguilar, G., Gray, A., Han, C., Bisignano, C., Rao, P., Wool, E., Johnson, S. C., Browne, A. J., Chipeta, M. G., Fell, F., Hackett, S., Haines-Woodhouse, G., Kashef Hamadani, B. H., Kumaran, E. A. P., McManigal, B., … Naghavi, M. (2022). Global burden of bacterial antimicrobial resistance in 2019: a systematic analysis. *The Lancet*, *399*(10325), 629–655. https://doi.org/10.1016/S0140-6736(21)02724-0

Nemeria, N., Yan, Y., Zhang, Z., Brown, A. M., Arjunan, P., Furey, W., Guest, J. R., & Jordan, F. (2001). Inhibition of the *Escherichia coli* pyruvate dehydrogenase complex E1 subunit and its tyrosine 177 variants by thiamin 2-thiazolone and thiamin 2-thiothiazolone diphosphates: evidence for reversible tight-bindı ng inhibition. *The Journal of Biological Chemistry*, *276*(49), 45969–45978. https://doi.org/10.1074/JBC.M104116200

Palla, G., Predieri, G., Domiano, P., Vignali, C., & Turner, W. V. (1986). Conformational behaviour and E/Z isomerization of N-acyl and N-aroylhydrazones. *Tetrahedron*, *42*(13), 3649–3654. https://doi.org/10.1016/S0040-4020(01)87332-4

Patel, M. S., & Korotchkina, L. G. (2003). The biochemistry of the pyruvate dehydrogenase complex. *Biochemistry and Molecular Biology Education*, *31*(1), 5–15. https://doi.org/10.1002/bmb.2003.494031010156

Patel, M. S., Nemeria, N. S., Furey, W., & Jordan, F. (2014). The pyruvate dehydrogenase complexes: Structure-based function and regulation. *The Journal of Biological Chemistry*, *289*(24), 16615–16623. https://doi.org/10.1074/jbc.R114.563148

Pires, D. E., Blundell, T. L., & Ascher, D. B. (2015). pkCSM: Predicting small molecule pharmacokinetic and toxicity properties using graphbased signatures. *Journal of Medicinal Chemistry*, *58*(9), 4066–4072. https://doi.org/10.1021/acs.jmedchem.5b00104

Rollas, S., & Küçükgüzel, Ş. G. (2007). Biological activities of hydrazone derivatives. *Molecules (Basel, Switzerland)*, *12*(8), 1910–1939. https://doi.org/10.3390/12081910

Sathisha, K. R., Khanum, S. A., Chandra, J. N. N. S., Ayisha, F., Balaji, S., Marathe, G. K., Gopal, S., & Rangappa, K. S. (2011). Synthesis and xanthine oxidase inhibitory activity of 7-methyl-2- (phenoxymethyl)-5H-[1,3,4]thiadiazolo[3,2-a]pyrimidin-5-one derivatives. *Bioorganic & Medicinal Chemistry*, *19*(1), 211–220. https://doi.org/10.1016/j.bmc.2010.11.034

Schrödinger, LLC. (2019). *Schrödinger release 2019-1: Maestro*. Schrödinger, LLC.

Sharma, S., Tyagi, T., Srivastava, M., Rani, K., Kumar, D., Asthana, S., & Raj, V. S. (2022). Identification and validation of potent inhibitor of *Escherichia coli* DHFR from MMV pathogen box. *Journal of Biomolecular Structure and Dynamics*, 1–10. https://doi.org/10.1080/07391102.2022.2080113

Şahin, A. F., Küçükgüzel, ŞG., & Akdemir, A. (2021). Molecular modelling studies to suggest novel scaffolds against SARS-CoV-2 target enzymes. *Journal of Research in Pharmacy*, *25*(6)(25(6), 1110–1117. http://dx.doi.org/10.29228/jrp.96

Şenkardeş, S., Erdoğan, Ö., Çevik, Ö., & Küçükgüzel, Ş. G. (2021). Synthesis and biological evaluation of novel aryloxyacetic acid hydrazide derivatives as anticancer agents. *Synthetic Communications*, *51*(17), 2634–2643. https://doi.org/10.1080/00397911.2021.1945105

Senkardes, S., & Kucukguzel, S. G. (2016). Recent progress on synthesis and anticancer activity of 4-thiazolidinone. *Mini-Reviews in Organic Chemistry*, *13*(5), 377–388. https://doi.org/10.2174/1570193X13666160826154159

Shawky, A. M., Abourehab, M. A. S., Abdalla, A. N., & Gouda, A. M. (2020). Optimization of pyrrolizine-based Schiff bases with 4-thiazolidinone motif: Design, synthesis and investigation of cytotoxicity and anti-inflammatory potency. *European Journal of Medicinal Chemistry*, *185*, 111780. https://doi.org/10.1016/j.ejmech.2019.111780

Testa, B., Crivori, P., Reist, M., & Carrupt, P. A. (2000). The influence of lipophilicity on the pharmacokinetic behavior of drugs: Concepts and

examples. *Perspectives in Drug Discovery and Design*, *19*(1), 179–211. https://doi.org/10.1023/A:1008741731244

Ullah, A., Iftikhar, F., Arfan, M., Batool Kazmi, S. T., Anjum, M. N., Haq, I. u., Ayaz, M., Farooq, S., & Rashid, U. (2018). Amino acid conjugated antimicrobial drugs: Synthesis, lipophilicity- activity relationship, antibacterial and urease inhibition activity. *European Journal of Medicinal Chemistry*, *145*, 140–153. https://doi.org/10.1016/j.ejmech.2017.12.089

Veber, D. F., Johnson, S. R., Cheng, H. Y., Smith, B. R., Ward, K. W., & Kopple, K. D. (2002). Molecular properties that influence the oral bioavailability of drug candidates. *Journal of Medicinal Chemistry*, *45*(12), 2615–2623. https://doi.org/10.1021/jm020017n

Verma, A., & Saraf, S. K. (2008). 4-Thiazolidinone - A biologically active scaffold. *European Journal of Medicinal Chemistry*, *43*(5), 897–905. https://doi.org/10.1016/j.ejmech.2007.07.017

Wolber, G., & Langer, T. (2005). LigandScout: 3-D pharmacophores derived from protein-bound ligands and their use as virtual screening filters. *Journal of Chemical Information and Modeling*, *45*(1), 160–169. https://doi.org/10.1021/ci049885e

Zhou, Y., Zhang, S., Cai, M., Wang, K., Feng, J., Xie, D., Feng, L., Peng, H., & He, H. (2021). Design, synthesis, and antifungal activity of 2,6-dimethyl-4-aminopyrimidine hydrazones as PDHc-E1 inhibitors with a novel binding mode. *Journal of Agricultural and Food Chemistry*, *69*(21), 5804–5817. https://doi.org/10.1021/acs.jafc.0c07701